Enzymatic Oxygen Microsensor Based on Bilirubin Oxidase Applied to Microbial Fuel Cells Analysis

Matteo Grattieri,[a, b] Sofia Babanova,[c] Carlo Santoro,[c] Edoardo Guerrini,[b] Stefano PM Trasatti,[b] Pierangela Cristiani,*[d] Massimiliano Bestetti,[a] and Plamen Atanassov*[c]

Received: September 26, 2014
Accepted: October 29, 2014
Published online: January 22, 2015

1 Introduction

Oxygen plays a key role in biofilm development and in biotechnologies based on microbial systems [1]. In the last twenty years Microbial Fuel Cell (MFC) has been one of the most attractive biotechnologies, since it has been demonstrated its capability to produce electricity directly from microbial oxidation of various organic compounds in wastewaters and wet wastes [2]. MFC is an electrochemical system that utilizes natural anaerobic degradation of organic matter in a particular way: using oxygen as a final electron acceptor at a cathode, avoiding the direct contact of oxygen with the other reactants confined in the anode compartment. The presence of oxygen at the anode can decrease significantly the kinetics of the involved processes and the efficiency of the electron transfer. It negatively influences the biofilm growth-rate, its morphology and bacteria diversity. Therefore, the diffusion of oxygen, especially in the case of membraneless systems, is an unwanted environmental factor, which should be diminished to negligible values if cannot be completely avoided. Conversely, the concentration of oxygen at the cathode needs to be maximized, as it is often the limiting reagent for efficient MFC operation [3–4].

Many and different configurations of MFC have been developed through the years in order to enhance the system performance and match the needs of various applications. Among them single chamber MFC in membraneless air-cathode configuration is gaining more and more attention, due to simple design and significant performance. In a membraneless MFC, biofilm can be grown on both of the electrodes, which allows mutual development of effective bio-anodes and bio-cathodes and the design of a complete MFC [5].

Since oxygen concentration is one of the main factors determining the single chamber MFC's performance, a selective and localized measurement of oxygen content is of primary importance for understanding the processes and the mechanisms involved in MFC operation [6]. Nevertheless, current MFC studies rarely report oxygen concentration measurements [7]. Most frequently, the presence/absence of oxygen is just supposed.

Commercial oxygen microsensors are relatively "cheap" in comparison to other advanced analysis techniques [8] but considering the cost of the equipment to use common microsensors, the price can be significant. Moreover, the characteristic application in MFCs of the existing microsensors is generally difficult due to the complex geometry of the cells. Therefore a hand-made microsensors with high selectivity and sensitivity has to be developed [9].

Enzymatic molecules are reported as highly active and selective towards a specific and unique reaction [10], which makes them useful for many industrial applications [11], as well as catalysts in the design of biofuel cells and biosensors [12–14]. The enzymatic microsensors have sev-

[a] M. Grattieri, M. Bestetti
Department of Chemistry, Materials and Chemical-Engineering, Politecnico di Milano
Piazza Leonardo Da Vinci, 32, 20133 Milan, Italy

[b] M. Grattieri, E. Guerrini, S. P. Trasatti
Department of Chemistry , Università degli Studi di Milano
Via Golgi 19, 20133 Milan, Italy

[c] S. Babanova, C. Santoro, P. Atanassov
Center for Emerging Energy Technologies, Department of Chemical & Nuclear Engineering, Center for Emerging Energy Technologies, University of New Mexico
Albuquerque, NM 87131, USA
*e-mail: plamen@unm.edu

[d] P. Cristiani
RSE – Ricerca sul Sistema Energetico S.p.A., Sustainable Development and Energy Sources Department
20133 Milan, Italy
*e-mail: pierangela.cristiani@rse-web.it

eral important features and the most important ones are selectivity and substrate specificity. Among the broad and diverse list of proteins, the enzymes belonging to the family of multi-copper oxidases (MCOs) are one of the most extensively studied and explored enzymes in the design of bio-electrochemical systems. This is mainly due to their capability for direct oxygen reduction to water, performing in nature and when incorporated in the design of enzymatic electrodes [15–17]. Bilirubin oxidase is an example of an MCO enzyme that oxidizes bilirubin to biliverdin with the concomitant reduction of O_2 to H_2O [18]. BOx contains three different copper centers (T1, T2 and T3), for a total of four copper atoms, classified depending on their magnetic and optical properties. The T1 site is the primary electron acceptor from the substrate or the electrode surface; the electrons are then transferred via an intramolecular electron transfer (IET) to the T2/T3 tri-nuclear cluster (TNC) constituted by a EPR active type II copper ion and a pair of type III cupric ions, responsible for the final O_2 reduction [19]. The capability of the BOx of exchange electrons at the electrode surface by direct electron transfer (DET) was repeatedly demonstrated using various carbonaceous electrodes [20,21]. Two possible electron-transfer mechanisms exist, by which MCOs can perform oxygen reduction reaction (ORR) at the electrode surface [15,16,20–22]:

i) A four-electron transfer

$$O_2 + 4H^+ + 4e^- \rightarrow 2H_2O \;\; 1.23\,\text{V vs. SHE} \qquad (1)$$

ii) Or a two-electron transfer producing hydrogen peroxide

$$O_2 + 2H^+ + 2e^- \rightarrow H_2O_2 \;\; 0.69\,\text{V vs. SHE} \qquad (2)$$

The formation of H_2O_2 decreases the number of electrons transferred per molecule of oxygen reacted and thus decreases the Columbic efficiency of the bioelectrode. In addition the produced H_2O_2 is toxic and can have negative impact on living cells. Consequently, for application of BOx in the design of amperometric microbiosensors for MFC monitoring, reaction (1) is the most favorable since it extracts the maximum number of electrons, increasing the recorded current and avoids the release of toxic products [15].

A key advantage of BOx and all MCOs is their ability to reduce oxygen by carrying out direct electron transfer avoiding the need of mediator utilization. In order to achieve DET, the enzyme active center should be placed in the proximity of the electrode surface. Various strategies have been proposed to promote DET [23]. One of them is modification of a carbon support with 1-pyrenebutyric acid, *N*-hydroxysuccinimide ester (PBSE), which provides stable and effective enzyme immobilization and DET [15]. The pyrene moiety of PBSE interacts with the aromatic-like structure of carbon materials through irreversible π–π stacking. This allows the functionalization of the electrode surface with succinimidyl ester groups that are highly reactive to nucleophilic substitution by primary and secondary amines that exist on the surface of the enzyme molecule [24,25]. PBSE-modified carbon cloth electrode was reported to support faster and more complete bio-electrochemical oxygen reduction than unmodified electrodes with only physisorbed BOx, generating higher current densities. According to Ramasamy [25] this effect can be related to the formation of a covalent bond between the amino group of the enzyme and the PBSE-tether that reduces the electron tunneling distance between the enzyme and the electrode, facilitating DET. Moreover it has been demonstrated that by cross-linking the enzyme to the electrode with PBSE, four-electron transfer mechanism of oxygen reduction reaction takes place (Equation 1) [15].

BOx displays high activity and stability at neutral pH and high tolerance towards different anions, such as F^- and Cl^- [26]. Therefore BOx has been used in physiological conditions as bilirubin or DNA sensor [27,28] and as catalyst for the ORR in biofuel cells including MFCs [20]. Constructing enzymatic oxygen microsensor based on the utilization of bilirubin oxidase will provide specific oxygen reduction avoiding the influence of other electrochemically active species, which is very likely to be present in wastewater or to be produced as intermediates or final metabolic products of organics oxidation during MFC operation.

The sensor demonstrated in this study is based on oxygen reduction catalyzed by bilirubin oxidase (BOx). The developed sensor was further explored for localized oxygen measurements, carried out in an operating MFC. Based on the sensor's readings an oxygen profile from the anode surface to the cathode and through the cathodic biofilm was created.

2 Experimental

2.1 Sensor Construction

A sheet of carbon cloth (Fuel Cell Earth) (Figure 1 A) was used as a source for the bundle of carbon cloth fibers (CC) (Figure 1 B) (average diameter for a bundle of fibers ≤ 100 μm; 10 μm single fiber diameter). The bundle (ohmic resistance between 6 and 10 Ω) was used as support for the construction of the enzymatic oxygen microsensor that at the end, as specified below, itself composed of only one fiber. In order to electrically connect and make the sensor more robust, the bundle of carbon cloth fibers was linked with a nickel wire (200 μm diameter) using a bi-component (A – monomer; B – hardener) silver conductive epoxy resin (H22 EPO-TEK) with a mixing ratio of 100A : 4.5B w/w. The volume resistivity of the paste is reported as $< 0.005\,\Omega\,\text{cm}$. Curing of the conductive epoxy resin was performed at 80 °C for 50 minutes. The obtained device (ohmic resistance between 15 and 30 Ω) was placed inside of a micropipette tip (200 μL Yellow Universal Pipette Tip, Figure 1 C) leaving only

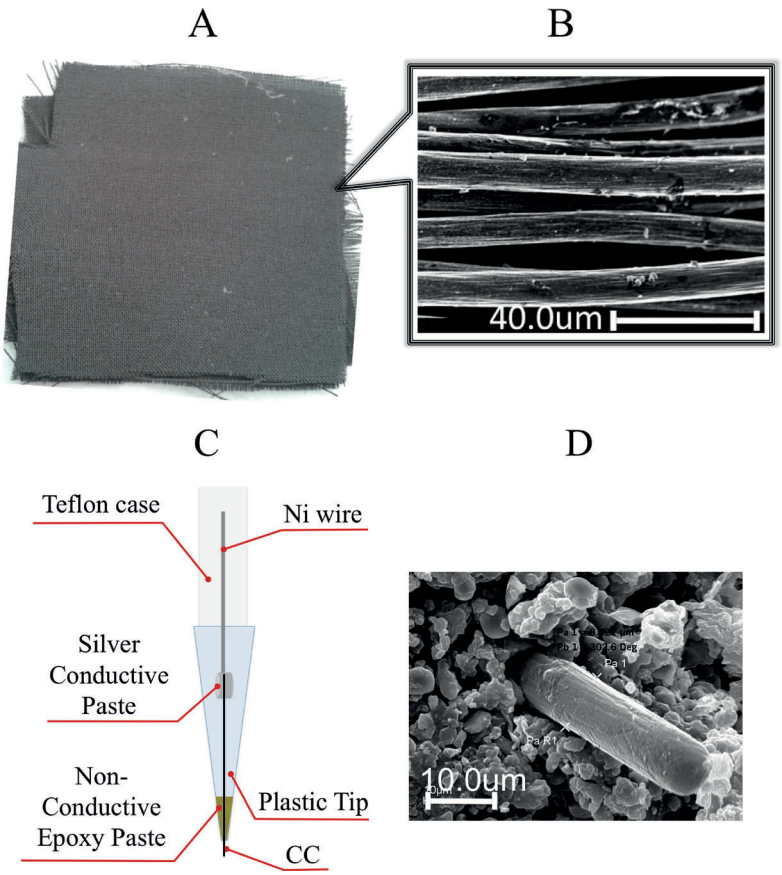

Fig. 1. Sensor construction. A) Carbon cloth sheet; B) SEM image of selected CC fibers bundle; C) schematic description of the device; D) SEM frontal view of a detail of the sensor tip before the lapping procedure.

one carbon fiber out of the tip at a certain extent. A bi-component nonconductive epoxy resin (3 M Scotch-Weld Epoxy Adhesive DP100 Clear) with a curing time of 8 hours at 25 °C was used to insulate the fiber and leave only the tip uncovered (Figure 1 D). The tip was then lapped with abrasive paper, thus the sensor exposed to the electrolyte was the end part of the single carbon fiber with a diameter of 10 μm (7.85×10^{-7} cm^2). Only this portion was further subjected to enzyme immobilization.

Bilirubin oxidase enzyme used in the present work was purchased from Amano Enzyme Inc. with a specific activity of 2.53 U/mg of protein. The enzyme was immobilized onto the carbon fiber surface via 1-pyrenebutyric acid, *N*-hydroxysuccinimide ester (PBSE, Sigma Aldrich).To accomplish that, the tip of the sensor was immersed in 0.01 M PBSE solution in dimethyl sulfoxide (DMSO) and left for 1 hour. The sensor was then washed, placed in 2 mg mL^{-1} solution of BOx, dissolved in 0.1 M phosphate buffer and kept at 4 °C for 16–18 hours to obtain enzyme attachment. After enzyme immobilization the biosensor was ready for calibration or further steps such as silica encapsulation.

To increase sensor stability and introduce diffusional barrier, the tip of the sensor was encapsulated using Chemical Vapor Deposition technique (CVD) as previously reported by Gupta et al. [29]. The silicate matrix was obtained by hydrolysis of tetramethyl orthosilicate (TMOS) as alkoxide precursor, followed by condensation to yield a polymeric oxo-bridged SiO_2 network. Encapsulated sensors were prepared by positioning the wet sensor after the enzyme immobilization in a closed petri dish with two small containers having 200 μL of tetramethyl orthosilicate (TMOS) and 200 μL of water, respectively, for five minutes at 30 °C. Only the liquid on the sensor surface is transformed into a silica gel. The additional water container serves to capture the excess of TMOS vapors.

2.2 Electrochemical Tests

A three-electrode setup was used for all electrochemical experiments, where the sensor was connected as working electrode (WE), a platinum wire was the counter electrode (CE) and a Ag|AgCl (3 M) electrode (3 mm diameter) was the reference electrode (+215 mV vs. SHE) (RE).

The electrochemical response of the device with and without immobilized BOx was studied by cyclic voltammetry at three different aeration conditions under controlled flow: air-saturated solution ([O_2 in solution] = 6.91 mg L^{-1}), 60 sec purging oxygen (purity 96 %, [O_2 in solution] = 20 mg L^{-1}) and 30 min purging nitrogen (purity

90 %, [O_2 in solution] = 0.66 mg L^{-1}). The cyclic voltammetry was recorded from 0.7 V to - 0.4 V vs. Ag|AgCl (3 M) (0.915 to −0.185 V vs. SHE) at 100 mV sec^{-1} in a 0.1 M phosphate buffer (PB) with 0.1 M KCl. Based on the performed CVs a potential of −0.4 V vs. Ag|AgCl (3 M) was selected for sensor calibration and operation.

The sensors were calibrated by chronoamperometry in three different aeration conditions: air-saturated solution ([O_2 in PB] = 6.91 mg L^{-1} and ([O_2 in WW] = 3.74 mg L^{-1}), 1 min purging nitrogen (purity 90 %, [O_2 in PB] = 5.47 mg L^{-1} and ([O_2 in WW] = 3.38 mg L^{-1}) and 30 min purging nitrogen ([O_2 in PB] = 0.66 mg L^{-1} and ([O_2 in WW] = 0.63 mg L^{-1}). The oxygen concentration in the calibration solutions was determined by a commercial DO probe (HQ440d, Hanch). Chronoamperometry is the most common technique used for the operation of amperometric sensors. It annihilates the influence of the capacitive current on the sensor reading and thus the performed measurement. The chronoamperometry was performed after 30 seconds of equilibration time with 120 seconds of current recording at −0.4 V vs. the Ag|AgCl (3 M) (−0.185 V vs. SHE). The current value was recorded every second and the steady state current observed at the end of the measurement was taken as the sensor reading. Calibration curves were obtained for both encapsulated and not encapsulated sensors in triplicate. The best performing sensor in terms of sensitivity and linearity of the response was chosen for monitoring a MFC system. The chosen sensor was further calibrated in wastewater using the same, previously described procedure in order to investigate an eventual matrix effect. The lifetime of the sensors was also studied. One and the same sensor was calibrated in wastewater at day one right after it has been prepared and then at different days (for example days 1, 3, 4, 5, 8 and 14). The sensor was kept at 4 °C between measurements.

2.3 MFC Setup

A membraneless single chamber MFC with gas-diffusion air-cathode, having a volume of 130 mL was used in this study. AISI 304L stainless steel anode [30] and activated carbon (AC) based cathode [31] were used as electrodes in the MFC. The electrolyte was urban wastewater coming from the treatment plant of Albuquerque (NM, USA). The wastewater was used as murky as received, without any pretreatment step. During MFC operation, sodium acetate (Sigma Aldrich) was added to the electrolyte as substrate (carbon source) for bacteria.

The MFC was polarized with a constant resistance (R) of 100 Ω and the cell voltage (V) across the resistance was monitored. V was recorded every 25 minutes, using a multichannel data logger (Personal DAQ/56). The current was calculated based on Ohm's law $I = V/R$ and power generation (P) was calculated using the formula $P = V \times I$.

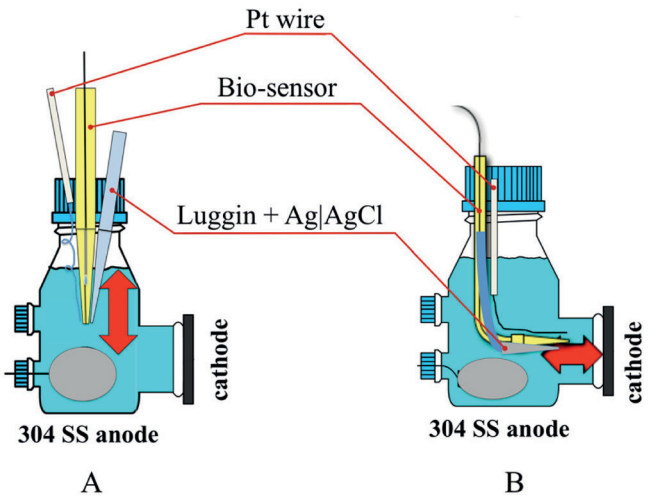

Fig. 2. Schematic analysis-setups. A) Approaching the anode, B) approaching the cathode.

2.4 Determination of Oxygen Profiles in MFC

In order to reduce eventual interference in the sensor response, profiles of oxygen concentration in proximity of both anode and cathode surfaces (Figures 2 A and 2 B, respectively) were determined under open circuit conditions of the MFC. Preliminary experiments (not reported here) demonstrated that the presence of a current flow could considerably increase the noise of the amperometric sensor response.

The microsensor along with Ag|AgCl (3 M) reference and Pt-wire counter electrodes were inserted from the upper cap of the MFC and moved down from the level of the solution towards the anode (Figure 2 A). For the cathode monitoring, the microsensor was bent to reach the cathode surface and it was moved from the anode towards the cathode creating oxygen profile between the two MFC electrodes (Figure 2 B). The position and movement of the oxygen microsensor was controlled by a computer-controlled stage (NLE Series Precision Linear Stage, Newmark Systems Inc.) having a maximum spatial resolution of 100 nm.

3 Results and Discussion

3.1 Electrochemical Performance

The electrochemical performance of the BOx-based microsensor was examined via cyclic voltammetry (CV), carried out at 100 mV s^{-1} in 0.1 M phosphate buffer + 0.1 M KCl solution (pH 7.5) (Figure 3). The potential window of the cyclic voltammetry was selected between 0.7 and −0.4 V vs. Ag|AgCl (3 M) (0.915 to −0.185 V vs. SHE) in order to avoid enzyme denaturation and ensure enzyme function. Control electrode, containing only carbon fiber and no enzyme showed almost flat response over the investigated potential window. After the enzyme immobilization, increased capacitance as well as current

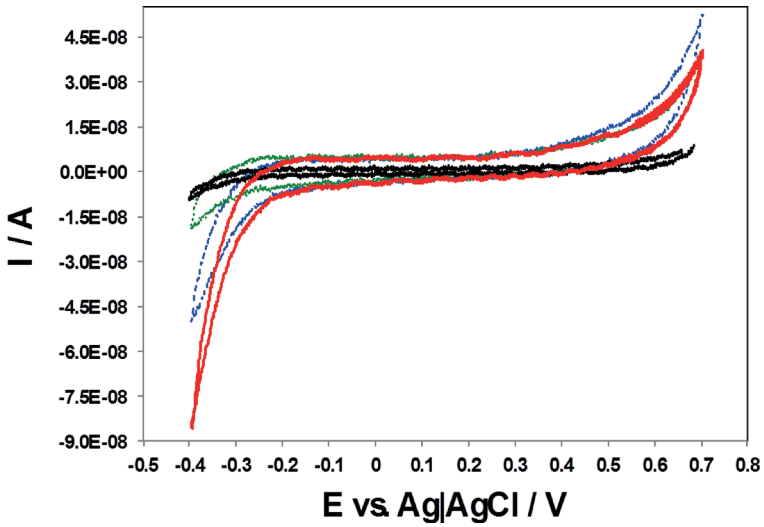

Fig. 3. CVs. Scan rate: 100 mV s^{-1}; CE: Pt; RE: Ag | AgCl (3 M). WE: carbon cloth fibers in oxygen saturated solution (black); BOx microsensor electrode (green) in oxygen depleted solution; BOx microsensor electrode (blue) in air-saturated solution and BOx microsensor electrode (red) in oxygen saturated solution.

output was observed. The highest difference in the sensor response as a result of different oxygen content in the electrolyte was recorded at −0.4 V vs. Ag | AgCl (3 M) (−0.185 V vs. SHE). Therefore potential of −0.4 V vs. Ag | AgCl (3 M) was consequently chosen as a proper potential for the subsequent chronoamperometry analyses.

One of the main problems of enzymatic biosensors and biological systems in general is their low stability. This constrain can be overcome with encapsulation of the enzyme in silica matrix [32]. Silica encapsulation is a simple, fast and effective method for entrapment of biological specimens. This encapsulation process involves low-temperature hydrolysis of appropriate monomeric precursors. The polymeric framework grows around the biomolecule, creating a cage and thus protecting the enzyme from aggregation and unfolding. These silica matrixes are chemically inert, hydrophilic, and inexpensive to synthesize. Their porous nature provides an efficient design that restricts movement of the enzyme but allows free access of the analytes [33]. In addition to the increased stability, the silica matrix creates a diffusional barrier, which ensures operation of the sensor at mass transport controlled mode and therefore has a linear response from the concentration of an analyte [34].

In order to test the effect of the silica layer on the performance of the developed enzymatic oxygen sensor, a comparison between encapsulated and not encapsulated sensors was also performed. Chronoamperometry measurements of the sensor response at various oxygen concentrations were carried out in 0.1 M phosphate buffer + 0.1 KCl solution at the chosen potential of −0.4 V vs. Ag | AgCl(3 M) (−0.185 V vs. SHE). These measurements were executed with two sensor types: type I: not encapsulated and type II: encapsulated with silica-layer enzyme. Each measurement was carried out in triplicate (Figures 4 A and 4 B).

Both sensor types showed a good linear current response as a function of oxygen concentration with a coefficient of determination $R^2 > 0.97$. The sensitivity of type I sensor was higher since the electrode was directly exposed to the electrolyte. At the same time, the reproducibility of the sensor response was lower in comparison to the encapsulated sensor (type II), especially at small oxygen concentrations, which we expect to have in MFCs. Therefore, the encapsulated sensor was selected for further implementation in determining MFC's oxygen profile due to its higher response reproducibility.

The next step was calibration of the type II (encapsulated) sensor in wastewater (WW) solution in order to avoid eventual matrix effect (Figure 4 C).

The sensor showed linear response in both PB and WW. The response in terms of current intensity and sensitivity was lower in the latter. There are two possible reasons for the decreased sensor performance: i) the conductivity of the wastewater is significantly lower than the phosphate buffer, which introduces ohmic losses and thus leads to decreased current densities; ii)although BOx is one of the enzymes from the family of MCOs that shows good resistance towards halogens, the complicated chemistry of the wastewater (used as received) creates a matrix effect that can modify the enzyme performances and behavior. Therefore, the MFCs analyses were performed after calibration of the sensor in WW solution. The presence of sludge in the murky solution did not affect the sensor linearity.

In order to study the sensor lifetime, the calibration procedure was repeated at different days (Figure 4 D). In terms of linearity and reproducibility the sensor performance was maintained for 8 days for the encapsulated biosensor. After that time, the response was no longer linear and became totally flat (Figure 4 D – Day 14). It is interesting to remark that the enzyme showed only slight

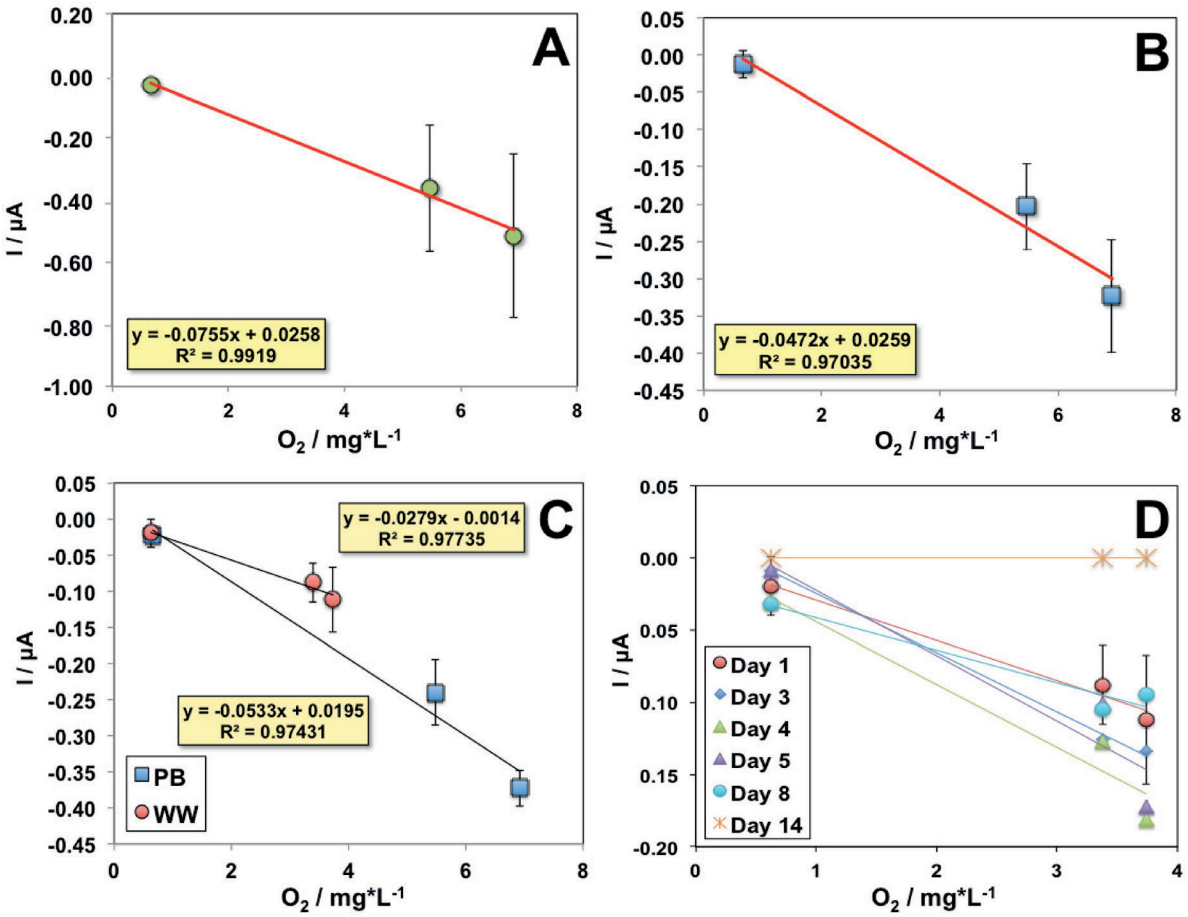

Fig. 4. Calibration curves. A) Not encapsulated sensor in 0.1 PB + 0.1 M KCl; B) encapsulated sensor in 0.1 PB + 0.1 M KCl; C) encapsulated sensor in 0.1 PB + 0.1 M KCl and in WW; D) lifetime in WW from day 1 to day 14.

gradual deactivation over time. The deactivation of the enzyme was faster for not encapsulated sensors: after 2–3 days unacceptable responses were obtained (data not shown). This phenomenon most likely was a consequence of the direct contact of the enzyme with pollutants in the wastewater that decreased significantly the enzymatic activity. Silica encapsulation stabilized the enzyme and quadrupled the sensor's life.

3.2 MFCs Analysis

Membraneless single chamber microbial fuel cell equipped with an activated carbon (AC) based gas-diffusion air-cathode and a stainless steel anode was inoculated with fresh urban wastewater at the beginning of the test. Sodium acetate was added to the electrolyte as a fuel source (3 g L^{-1}) for bacteria. The MFC was polarized with a constant resistance of 100 Ω and the corresponding cell voltage was recorded and recalculated in terms of power. The power generated form the MFC over time is shown in Figure 5.

The MFC was unproductive for five days, as power values close to zero were observed. At day 6, the cell started to produce power, reaching 0.01 mW, which dropped to zero at day 7. At the end of day 9, the 3 g L^{-1} sodium acetate concentration was re-established by addition of acetate in the solution. Three days later (day 12), the power production started again and constantly increased until day 18 (0.08 mW), when the experiment was terminated.

3.2.1 Oxygen Profiles Towards the Anode Surface

Profiles of oxygen concentration in the proximity of the anode were determined under MFC open circuit conditions. The microsensor was inserted into the MFC and moved down from the level of the solution to the anode surface (Figure 2 A). The position of the oxygen microsensor was controlled by a computer-controlled stage with a maximum spatial resolution of 100 nm. The oxygen profiles approaching the anode surface were measured at different time intervals: after day 1, 3, 8 and 15 of MFC operation (Figure 6 A).

At the startup of the MFC operation (day 1), the oxygen concentration was approximately constant along the entire path, with the exception of the first millimeters close to the solution surface where the concentration of oxygen was higher. After 3 days, the concentration was

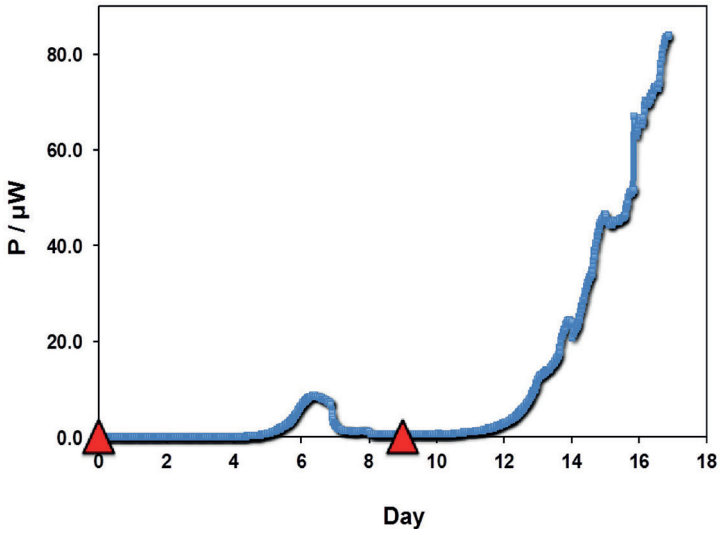

Fig. 5. Power generated by the SCMFC over time. Triangles indicate acetate addition.

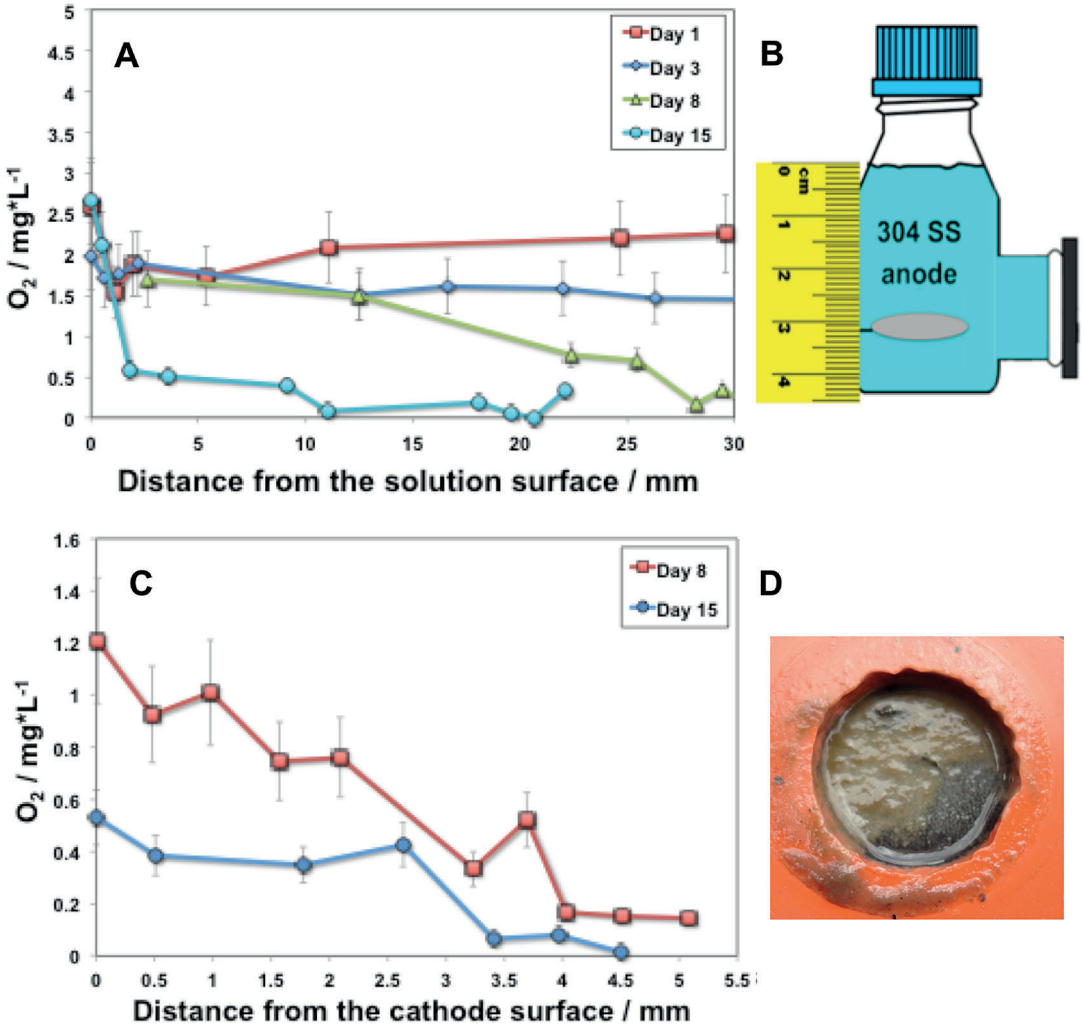

Fig. 6. A) Oxygen profile to the anode surface at days 1, 3, 8 and 15; B) schematic depth indicator; C) oxygen profiles to the cathode surface at days 8 and 15; D) cathodic biofilm after 18 days of operation.

still constant but at a slightly lower value. The oxygen consumption during these first days is associated with the microbial aerobic processes taking place in the anodic chamber of the MFC during the startup process with no power production. As a result of oxygen consumption, anaerobic conditions establish inside the bulk solution, from the solution surface towards the proximity of the anode [35]. The lower oxygen concentration detected in the MFC at day 8 shows that oxygen was progressively consumed over this period. The MFC started to produce power at day 6, and when all the acetate was consumed, it fell dramatically to zero. A very low oxygen concentration at 10 mm from the solution surface was detected at day 15, consistent with the highest power production. These results remark that the absence of oxygen in the region close to the anode of the MFC plays a key role in the cell productivity and that the designed herein enzymatic microsensor can be successfully explored to study the changes in oxygen content as a function of the distance from the anode surface.

3.2.2 Oxygen Profiles Towards the Cathode Surface

For the cathode analyses, the microsensor was moved from the anode towards the cathode (Figure 2B). The oxygen profiles measured approaching the cathode surface are shown in Figure 6C at two different days (8 and 15).

The oxygen content at 4.5 mm far away from the cathode surface was almost equal to that measured close to the anode at the same days of MFC operation. Moving the sensor closer to the cathode surface, the oxygen concentration tended to increase with a different slope, higher at day 15. At day 8, oxygen continuously increased towards the electrode surface, reaching 1.2 $mg\,L^{-1}$ in the proximity of the cathode. The curve at day 15 exhibits a practically flat profile from 2.5 mm to the cathode surface, where the oxygen content was 0.6 $mg\,L^{-1}$. This concentration was half of value observed for day 8.

The results confirm that the biofilm developed at the cathode surface (figure 6D) acts as barrier for oxygen diffusion, as previously hypothesized [5,7,36] and further demonstrates that the power production was strictly connected to the oxygen consumption in the MFC. Based on the oxygen-profile measurements it can be proposed that the cathode biofilm has a thickness around 3 mm.

4 Conclusion

An enzymatic microsensor based on bilirubin oxidase was built up, calibrated and utilized to measure oxygen content in a membraneless MFC.

Three relevant points demonstrate the effectiveness of the microsensor:

a. The sensor has linear response for oxygen concentration;

b. It is not poisoned by wastewater;

c. The encapsulation step with TMOS provided a diffusional barrier improving reproducibility and stability of the sensor.

The utilization of low-cost materials, the shape of the sensor suitable for different MFC configurations and its extreme selectivity permit its application to several bioelectrochemical systems, not limited to MFCs.

Acknowledgements

This work has been supported by the Research Fund for the Italian Electrical System under the Contract Agreement between RSE and the *Ministry of Economic Development and General Directorate for Nuclear Energy, Renewable Energy and Energy Efficiency* and by the *UNM Center for Emerging Energy Technologies.*

References

[1] P. S. Stewart, *J. Bacteriol.* **2003**, *185*, 1485–1491.

[2] B. E. Logan, P. Aelterman, B. Hamelers, R. Rozendal, U. Schröeder, J. Keller, S. Freguia, W. Verstraete, K. Rabaey, *Environ. Sci. Technol.* **2006**, *40*, 5181–5192.

[3] G. G. Andeson, G. A. O'Toolein, *Bacterial Biofilms* (Ed: T. Romero), Springer, Heidelberg, **2008**, pp. 85–91.

[4] B. Capdeville, K. M. Nguyen, J. L. Rols, in *Biofilms – Science and Technology* (Eds: L. F. Melo, T. R. Bott, M. Fletcher, B. Capdeville), Kluwer Academic Publishers, Amsterdam, The Netherlands, **1992**, pp. 251–276.

[5] P. Cristiani, M. L. Carvalho, E. Guerrini, M. Daghio, C. Santoro, B. Li, *Bioelectrochemistry* **2013**, *92*, 6–13.

[6] G. T. Babauta, H. D. Nguyen, O. Instanbullu, H. Beyenal, *Chem. Sus. Chem.* **2013**, *6*, 1252–1261.

[7] C. Santoro, M. Cremins, U. Pasaogullari, M. Guilizzoni, A. Casalegno, A. Mackey, B. Li, *J. Electrochem. Soc.* **2013**, *160*, G3128–G3134.

[8] N. P. Revsbech, *Meth. Enzymol.* **2005**, *397*, 147–166.

[9] C. C. Wu, T. Yasukawa, H. Shiku, T. Matsue, *Sens. Actuators B* **2005**, *110*, 342–349.

[10] L. Hedstrom, in *Enzyme Specificity and Selectivity*, Elsevier, Amsterdam, **2010**.

[11] O. Kirk, T. V. Borchert, C. C. Fuglsang, *Curr. Opin. Biotech.* **2002**, *13*, 345–351.

[12] E. J. Calvo, A. Wolosiuk, *ChemPhysChem* **2005**, *6*, 43–47.

[13] N. G. Tognalli, P. Scodeller, V. Flexer, R. Szamocki, A. Ricci, M. Tagliazucchi, E. J. Calvo, A. Fainstein, *PhysChemChemPhys* **2009**, *11*, 7412–7423.

[14] D. Ivnitski, P. Atanassov, C. Apblett , *Electroanalysis* **2007**, *19*, 1562–1568.

[15] S. Broncato, C. Lau, P. Atanassov, *Electrochim. Acta* **2012**, *61*, 44–49.

[16] R. D. Milton, F. Giroud, A. E. Thumser, S. D. Minteer, R. T. C. Slade, *Chem. Commun.* **2014**, *50*, 94–96.

[17] R. Szamocki, V. Flexer, L. Levin, F. Forchiasin, E. J. Calvo, *Electrochim. Acta* **2009**, *54*, 1970–1977.

[18] N. Tanaka, S. Murao, *Agric. Biol. Chem.* **1985**, *49*, 843–844.

[19] E. I. Solomon, U. M. Sandaram, T. E. Machonkin, *Chem. Rev.* **1996**, *96*, 2563–2605.

[20] G. Gupta, C. Lau, V. Rajendran, F. Colon, B. Branch, D. Ivnitski, P. Atanassov, *Electrochem. Commun.* **2011**, *13*, 247–249.

[21] S. Shleev, J. Tkak, A. Christenson, T. Ruzgas, A. I. Yaropolov, J. W. Whittaker, L. Gorton, *Biosens. Bioelectron.* **2005**, *20*, 2517–2554.
[22] S. C. Barton, H. H. Kim, G. Binyamin, Y. Zhang, A. Heller, *J. Phys. Chem. B* **2001**, *105*, 11917–11921.
[23] P. Ramirez, N. Mano, R. Andreu, T. Ruzgas, A. Heller, *Biochim. Biophys. Acta* **2008**, *1777*, 1364–1369.
[24] R. J. Chen, Y. Zhang, D. Wang, H. Dai, *J. Am. Chem. Soc.* **2001**, *123*, 3838–3839.
[25] R. P. Ramasamy, H. R. Luckarift, D. Ivnitski, P. Atanassov, G. R. Johnson, *Chem. Commun.* **2010**, *46*, 6045–6047.
[26] J. Hirose, K. Inoue, H. Sakuragi, M. Kikkawa, M. Minakami, T. Morikawa, H. Iwamoto, K. Hiromi, *Inorg. Chim. Acta* **1998**, *273*, 204–212.
[27] B. Shoham, Y. Migron, A. Riklin, I. Willner, B. Tartakovsky , *Biosens. Bioelectron.* **1995**, *10*, 341–352.
[28] Y. Zhang, A. Pothukuchy, W. Shin Y. Kim, A. Heller, *Anal. Chem.* **2004**, *76*, 4093–4097.
[29] G. Gupta, S. B. Rathod, K. W. Staggs, L. K. Ista, K. A. Oucherif, P. Atanassov, M. S. Tartis, G. A. Montaño, G. P. López, *Langmuir* **2009**, *25*, 13322–13327.
[30] E. Guerrini, P. Cristiani, M. Grattieri, C. Santoro, B. Li, S. P. Trasatti, *J. Electrochem. Soc.* **2014**, *161*, H62–H67.
[31] C. Santoro, K. Artyushkova, S. Babanova, P. Atanassov, I. Ieropoulos, M. Grattieri, P. Cristiani, S. P. Trasatti, B. Li, A. J. Schuler, *Biores. Tech.* **2014**, *163*, 54–63.
[32] D. Avnir, S. Braun, O. Lev, M. Ottolenghi, *Chem. Mater.* **1994**, *6*, 1605–1614.
[33] J. K. McIninch, E. R. Kantrowitz, *Biochim. Biophys. Acta* **2001**, *1547*, 320–328.
[34] J. R. Stetter, W. R. Penrose, S. Yao, *J. Electrochem. Soc.* **2003**, *150*, S11–S16.
[35] E. Guerrini, P. Cristiani, S. P. Trasatti, *J. Hydr. Energ.* **2013**, *38*, 345–353.
[36] E. Guerrini, M. Grattieri, S. P. Trasatti, M. Bestetti, P. Cristiani, *J. Hydr. Energ.* **2014**, *39*, 21837–21846.